Spatio-temporal variability of zooplankton standing stock in eastern Arabian Sea inferred from ADCP backscatter measurements

Ranjan Kumar Sahu, P. Amol, D.V. Desai, S.G. Aparna, D. Shankar

June 13, 2024

Abstract

We use acoustic Doppler current profiler (ADCP) backscatter measurements to map the spaio-temporal variation of zooplankton standing stock in the eastern Arabian Sea (EAS). The ADCP moorings were deployed at seven locations on the continental slope off the west coast of India; we use data from October 2017 to December 2023. The 153.3 kHz ADCP uses backscatter from sediments or organisms such as copepods, ctenophores, salps and amphipods greater than 1 cm to calculate current profile. The backscatter is obtained from echo intensity using RSSI conversion factor after doing necessary calibrations. The conversion from backscatter to biomass is based on volumetric zooplankton sampling at the respective locations. Analysis of the data over 24 – 120 m shows that the backscatter and zooplankton biomass decrease from the upper ocean (215 $m\ g^{-3}$ biomass contour) to the lower depths. Changes are observed in the seasonal variation of the monthly

climatology of zooplankton standing stock (integral of the biomass over 24 – 120 m water column) as we move to poleward along the slope in EAS. The range of variation of standing stock is lowest at Kanyakumari, followed by Okha, which lie at the southern and northern boundary of the EAS, respectively. Complementary variables are used to explain the processes leading to growth or decay of zooplankton biomass.

1 Introduction

1.1 Background

Zooplankton plays a vital role in food web of pelagic ecosystem by enabling the hierarchical transport of organic matter from primary producers to higher trophic levels impacting the fish population and the carbon pump of the deep ocean [Ohman and Hirche, 2001, Le Qu et al., 2016]. They are presumably the largest migrating organisms in terms of biomass [Hays, 2003] which occurs in Diel Vertical Migration (DVM). Zooplanktons depend not only on phytoplankton but other environmental parameters (e.g. Mixed layer depth, insolation, Oxygen, thermocline, nutrient availability, chlorophyll concentration and daily primary production). The biological productivity of the ocean is essentially connected with physics and chemistry [Subrahmanyan, 1959, Ryther et al., 1966, Qasim, 1977, Nair, 1970, Banse, 1995, McCreary et al., 2009, Vijith et al., 2016, Amol et al., 2020]. The dynamic ocean results in varying physico-chemical properties, leading to bloom and growth of planktons in favourable conditions. The changes are strongly influenced by the seasonal cycle in the North Indian Ocean (NIO; north of $5\ ^{o}$N of Indian Ocean). The eastern boundary of Arabian Sea contains the West India Coastal Current (WICC; [Patil et al., 1964, Ramamirtham and Murty, 1965, Banse, 1968, Shetye et al., 1991, McCreary Jr et al., 1993, Shankar and Shetye, 1997, Shetye and Gouveia, 1998, Maheswaran et al., 2000, Amol et al., 2014, Chaudhuri et al., 2020, 2021]) which reverses seasonally, flowing poleward (equator-ward) during November to February (June to September).

The direct consequence of this reversal is the seasonal cycle of thermocline, oxycline and thickness of mixed Layer Depth (MLD) induced by upwelling favourable conditions in summer and downwelling favourable conditions in winter in eastern Arabian Sea (EAS). Further, the phytoplankton biomass and chlorophyll concentration changes with the season [Subrahmanyan and Sarma, 1960, Banse, 1968, Lévy et al., 2007, Vijith et al., 2016]. Upwelling in summer monsoon leads to maximum chlorophyll growth in the entire EAS [Banse, 1968, Banse and English, 2000, McCreary et al., 2009, Hood et al., 2017]. During winter monsoon, the convective mixing induced winter mixed layer [Shetye et al., 1992, Madhupratap et al., 1996b, Lévy et al., 2007, Vijith et al., 2016, Shankar et al., 2016, Keerthi et al., 2017] results in winter chlorophyll peak in northern EAS (NEAS) while the downwelling Rossby waves modulate chlorophyll along the southern EAS (SEAS) albeit limited to coast and islands [Amol et al., 2020]. (For a detailed description on EAS division, please refer figure 1 of [Shankar et al., 2019].

The zooplankton grazing peak is instantaneous with no time delay from peak phytoplankton production [Li et al., 2000], but its population growth lags [Rehim and Imran, 2012, Almén and Tamelander, 2020] depending on its gestation period and other limiting aspects. While some studies suggest that the peak timing of zooplankton may not change in parallel with phytoplankton blooms [Winder and Schindler, 2004], others indicate that lag exists between primary production and the transfer of energy to higher trophic levels [Brock and McClain, 1992, Brock et al., 1991]. A recent work [Aparna et al., 2022] had shown that peak zooplankton population may never occur even with a bloom in phytoplankton such as in SEAS, leading to the collapse of ecological models and succeeding food webs of higher trophic levels.

The conventional zooplankton measurements, where only few snapshot/s of the event is captured gives an incoherent or incomplete understanding in terms of spatio-temporal variation of zooplankton [Ramamurthy, 1965, Piontkovski et al., 1995, Madhupratap et al., 1992, 1996a, Wishner et al., 1998] as much information is revealed by later studies [Jyothibabu et al., 2010, Vijith et al., 2016, Shankar et al., 2019, Aparna et al., 2022] using high resolution data. Calibrated acoustic instruments such as Acoustic Doppler Current Profiler (ADCP) along with relevant data can be utilised to understand small scale variability [Nair et al., 1999, Edvardsen et al., 2003, Smith and Madhupratap, 2005, Smeti et al., 2015, Kang et al., 2024], the complex interplay between the physico-chemical parameters and ecosystem [Jiang et al., 2007, Potiris et al., 2018, Shankar et al., 2019, Aparna et al., 2022, Nie et al., 2023], the zooplankton migration [Inoue et al., 2016, Ursella et al., 2018, 2021] and their seasonal to annual variation [Jiang et al., 2007, Hobbs et al., 2021, Liu et al., 2022, Aparna et al., 2022].

1.2 ADCP backscatter and zooplankton biomass

At present, there are two types of acoustic samplers: non-calibrated single frequency acoustic profiler such as ADCP or calibrated multi and mono frequency acoustic profilers such as zooplankton acoustic profiler (ZAP) and Tracor acoustic profiling system(TAPS). The use of acoustics as a proxy for zooplankton biomass estimation can be traced to [Pieper, 1971, Sameoto and Paulowich, 1977] and earlier studies which used echograms to approximate the large-scale horizontal extents [Barraclough et al., 1969], and small scale vertical extent [McNaught, 1968]. The relationship between backscatter and the abundance and size of zooplankton was described by [Greenlaw, 1979] wherein it was pointed out that single frequency backscatter can be used to estimate abundance if mean zooplankton size is known. This paved the way for use of single frequency acoustic profiler. A drastic increase in study temporal and spatial variation of zooplankton biomass using backscatter-proxy came in 1990s by introduction of high frequency echo sounders, with studies [Flagg and Smith, 1989, Wiebe et al., 1990, Batchelder et al., 1995, Greene et al., 1998, Rippeth and Simpson, 1998] methodically showing acoustic backscatter estimated zooplankton biomass in various shelf and slope locations around North Atlantic, North pacific location. The foundation for further research that investigated the potential of acoustic backscatter from ADCPs and multi frequency echo sounders in assessing zooplankton biomass and comprehending zooplankton dynamics in diverse maritime habitats was established by these initial explorative experiments.

Acoustic backscatter and zooplankton biomass have been better understood as a result of technological and methodological developments over time. Net sampling augmented ADCP backscatter have been used to study DVM and the spatial and temporal variability of zooplankton biomass by [Cisewski et al., 2010, Smeti et al., 2015, Guerra et al., 2019] in different marine regions, such as the Southwestern Pacific, the Lazarev Sea in Antarctica and the Corsica Channel in the north-western Mediterranean Sea. The zooplankton biomass variation in the Arabian sea has been studied during JGOFS programme in 1990s [Herring et al., 1998, Nair et al., 1999, Fielding et al., 2004, Smith and Madhupratap, 2005]. However, their studies were limited to the cruise duration as vessel mounted ADCPs were predominantly used; hence long-term data was sparsely produced. The first such study to fully exploit the immense potential of ADCPs in EAS was carried out by [Aparna et al., 2022] using ADCP moorings deployed on continental slopes off the Indian west coasts [Amol et al., 2014, Chaudhuri et al., 2020].

1.3 Objective and scope of the manuscript

A network of ADCPs has been installed off the continental slope and shelf on the west coast of India. This ADCPs have enabled a rigorous view of intraseasonal to seasonal scale variability [Amol et al., 2014, Chaudhuri et al., 2020]. Initially a network of 4 ADCPs (off Mumbai, Goa, Kollam and Kanyakumari) on continental slope, it has been extended to include 3 more moorings (off Okha from 2018, Jaigarh and Udupi from 2017). In the recent study [Aparna et al., 2022] have used ADCP moorings off Mumbai, Goa and Kollam to explain the temporal variability of zooplankton biomass.

The study showed that the zooplankton peaks (and troughs) is not only non-uniform in latitude but also heavily influenced by the oxygen minimum zone, MLD and the seasonal upwelling/downwelling conditions. Stark contrast in the phytoplankton bloom and subsequence growth of zooplankton or the lack thereof was observed in the EAS regimes.

We build upon the existing work by extending to include the newly incorporated ADCPs so as to have a better understanding in the latitudinal variation of zooplankton biomass in EAS. The paper is organized as follows; datasets and methods employed are described in detail in Section 2. Section 3 describes the observed climatology of zooplankton biomass and standing stock. A comparison is drawn to the results of previous studies at the overlapping mooring sites. Further, the seasonal cycle of zooplankton biomass and standing stock is discussed. The role of mixed layer depth, net primary production, sea surface temperature, wind forcing and circulation in determining the biomass is discussed in results section 4, with conclusion in section 5.

2 Data and methods

The backscatter data from ADCP and the zooplankton samples collected from the periphery of mooring is described in this section. The methodology followed in processing ADCP data and estimation of backscatter and subsequently the zooplankton biomass is discussed. The backscatter derived from the echo intensity of the seven ADCP mooring deployed on the continental slope off the Indian west coast is the primary data we have use in this manuscript. The moorings details are summarised in Table1. In situ biomass data from volumetric zooplankton samples are used to validate and correlate with backscatter. The chlorophyll data is obtained from marine.copernicus.eu. In addition, we have used the monthly climatology of temperature and salinity [Chatterjee et al., 2012] and the net primary productivity from MODIS (Moderate Resolution Imaging Spectroradiometer) and VIIRS (Visible Infrared Imaging Radiometer Suite) from global NPP estimates (http://sites.science.oregonstate.edu/ocean.productivity).

2.1 ADCP data and Backscatter estimation

The ADCPs were deployed on the continental slope off the Indian west coast. Initially a set of three ADCPs, it was gradually extended to four more sites to cover the entire EAS basin from Okha (22.26^{o}N) in north to Kanyakumari (6.96 ^{o}N) in south. The other two ADCPs are Jaigarh at central EAS (CEAS) and Udupi in the transition zone between CEAS & SEAS. The extended moorings were deployed in October 2017, except for Kanyakumari which was deployed earlier as well but it wasn't included in earlier backscatter study. The moorings are serviced on yearly basis usually during October-November or in winter monsoon months. The ADCPs are of RD Instruments make, upward-looking and operate at 153.3 kHz. While utmost care is taken to position the instrument at $\sim$ 200 m depth, yet for some deployments it's shallow or deeper owing to drift caused by floater buoyancy - anchor weight balance. Data was collected at hourly interval and the bin size was set to 4 m. The echoes at surface to 10 % range (20 m) means the data at these is rendered useless and is discarded from further use.

The procedure followed in processing of the ADCP data are described in [Amol et al., 2014] and [Mukherjee et al., 2014]. An addition to their methodology was to do depth correction to accommodate the vertical movement of ADCP buoys [Chaudhuri et al., 2020, Mukhopadhyay et al., 2020] using data from pressure sensor mounted on the instrument. We have followed the methodology laid down in [Aparna et al., 2022] to derive the backscatter time series from ADCP echo intensity data which is discussed later paragraph. The gaps are filled using the grafting method of [Mukhopadhyay et al., 2020] once the zooplankton biomass time series is constructed.

The primary objective of ADCP usage is to obtain vertical current profile at a point location. It is achieved by using the echo intensity received at the ADCP transducer. The instrument sensors doesn't directly give backscatter, as echo intensity is range independent. Range correction has to be performed before echo intensity (E) is converted to Backscatter (B). Received signal strength indicator (RSSI), also called the conversion factor (Kc) which is specific to a sensor is used along with the corresponding reference echo intensity (Er). It's important to state that for the same device Kc remains unchanged while Er varies over each subsequent deployment. The backscattering strength (in dB) is given by [Mullison, 2017]:

$$B = [C - L_{DBM} - P_{DBW}] + 2\alpha R + 10log_{10}[(T_{TD} + 273.16)R^2] + 10log_{10}[10^{K_c(E-E_r)/10} - 1]$$

where C is an empirical constant, L_{DBM} is $10log_{10}L$ where L is the transmit pulse length in meters, P_{DBW} is $10log_{10}P$ (P is transmitted power in watts), α is the sound absorption coefficient of water (in $dB\ m^{-1}$), T_{TD} is the temperature (in $^o\ C$) at the depth of positioned instrument, R is the slant range (in meters) from transducer to the scatterers and E_r is the reference level of E taken in real-time (unit counts). E_r in our case is taken from first (last) measured profile when the instrument is in air before (after) deployment (retrieval). The backscattering strength is referenced to $(4\pi m^{-1})$ [Deines, 1999, Mullison, 2017]. Aparna et al. [2022] has discussed the relevance of each of the term to the total backscattering strength. Our analysis also suggests that the α does not affect the final results.

2.2 Zooplankton data and estimation of biomass

The zooplankton samples were collected in the vicinity ($\sim$ 10 km) of ADCP mooring site twice; once prior retrieval and again post deployment of moorings so that there is overlap in the ADCP time instance and in situ zooplankton samples. The sampling is done at the mooring location during servicing cruises on board RV Sindhu Sankalp and RV Sindhu Sadhana (Table 2). Multi-plankton net (MPN) (100 μm mesh size, 0.5 m^2 mouth area) was used to get samples in the pre-determined depth ranges; water volume filtered was calculated by the product of sampling depth range and the mouth area of net. The depth range and timing of sample collection was different throughout the MPN hauls. From 2020 onwards, the depth-range was standardised to the bins of 0 - 25, 25 - 50, 50 - 75, 75 - 100, 100 - 150 (units are in meters). The collected zooplankton samples were then preserved in 5 % formaldehyde solution until it's transferred to laboratory. To measure zooplankton wet weight accurately, the gelatinous forms/salps were separated. [Aparna et al., 2022] had reposted the calanoid copepods, cyclopoid copepods, Poecilostomatoida, Harpacticoida, appendicularians, euphausids, ostracods, and chaetognaths as the major groups of zooplankton s contributing to the biomass of net samples from the mooring sites this has to be updated to include later samples. The backscatter obtained earlier is averaged in vertical corresponding to the specific MPN hauls for each site. The backscatter is linear regressed with respective biomass to establish their relationship, which has been demonstrated in numerous previous studies [Flagg and Smith, 1989, Heywood et al., 1991, Jiang et al., 2007, Aparna et al., 2022].

We calculated the regression equation to be $y = 0.0203\ x + 4.01$ and, which is well within the error range of the regression equation of [Aparna et al., 2022], $y = (0.02 \pm 0.004)\ x + (4.14 \pm 0.36)$ with a correlation of 0.53. The correlation value in our case is 0.54; the minor difference is due to higher number of data points (159) in the present study.

2.3 Biomass time series and estimation of standing stock

The zooplankton biomass time series is created from the above derived linear relationship: $\log_{10}(\text{biomass}) = m * \text{Backscatter} + k$, where m is slope and k is intercept. The time series shows the pattern of diel vertical migration (DVM) at all the mooring sites during dawn (∼0600-0700 hours) and dusk (∼1800-1900 hours). It is evident in earlier studies using backscatter [Ashjian et al., 2002, Smith and Madhupratap, 2005, Inoue et al., 2016, Ursella et al., 2018] and in situ zooplankton data [Padmavati et al., 1998]. The implication of DVM is a higher biomass at surface during the night as zooplankton feeds and a lower biomass at daytime as they descend to subsurface depths. The overall biomass over the time period of a day may vary but the DVM doesn't affect the seasonal variation as shown by ([Jiang et al., 2007, Aparna et al., 2022]). Since our goal is to study the seasonal variation, delineating the daily biomass is sufficient. The biomass time series is discussed in section **name the section 3.1?**.

The standing stock is determined by taking the depth integral of biomass. To maintain the consistency of standing stock estimation, only those deployments that doesn't lack data at any depth in the entire range of 24 - 120 m are considered for analysis. The lack of data in the above mentioned depth range is due to deviation in positioning of ADCP sensor in the water column. A swift alteration in bathymetry along the continental slope implies that the mooring might anchor at a different depth than planned, hence a change in the predicted position of ADCP. This leads to gap in data at few mooring sites for some year. For example, for the northern-most mooring at Okha, data is not available for the entire upper 120 m depth for the second deployment. Also at Jaigarh, where the surface to ∼60m data (in 3rd deployment) and Kollam, where 80 m and below (in 4th deployment) is unavailable and hence discarded from standing stock estimation. There are few deployments where no data or bad data was recorded e.g, at Udupi (4th deployment) and Kanyakumari (6th deployment). The seasonal cycle of standing stock for 24 - 120 m available data is explored in section **name of the section, 3.2?**.

2.4 Chlorophyll and net primary productivity data

Previous study based on ADCP data of EAS [Aparna et al., 2022] have used SeaWIFS based chlorophyll data for comparison with climatology of zooplankton standing stock (ZSS). The SeaWIFS was at its end of service in 2010, hence we use new chlorophyll product. The present study has been conducted using Global Ocean Colour, biogeochemical, L3 data obtained from the E.U. Copernicus Marine Service Information. The daily data is available at a spatial resolution of 4 km.

While chlorophyll is used to compare with the variation in climatology of zooplankton standing; the growth efficiencies of zooplankton are directly linked to primary production levels, emphasizing the interconnectedness between primary producers and consumers in marine food webs [Friedland et al., 2012]. In their study, [Aparna et al., 2022] has emphasised on the collapse of the predator-prey relationship between zooplankton-phytoplankton using climatological data. We showcase their interdependency or the lack thereof using net primary productivity models. Moderate Resolution Imaging Spectroradiometer (MODIS) based net primary productivity (NPP) data at a resolution of 0.16^o x 0.16^o was obtained from Oregon State University. They have employed three different schemes to obtain NPP from Chlorophyll concentration. Those are discussed below in brief. The first is Vertically Generalized Production Model (VGPM). The NPP (a rate term) is to be derived from chlorophyll (a standing stock) using chlorophyll-specific assimilation efficiency for carbon fixation. The single biggest unknown in all models based on chlorophyll is how this rate term is described. VGPM considers the primary productivity to be dependent on day length and maximum daily NPP within a water column. The second is Carbon-based Productivity Model (CbPM) which NPP to phytoplankton carbon biomass and growth rate. The third is Carbon, Absorption, and Fluorescence Euphotic-resolving (CAFE) mode; first described by [Silsbe et al., 2016] takes various other factors into NPP calculations. We explore these NPP models and try to explain the variation in ZSS.

3 Climatology of zooplankton biomass and standing stock

The previous study of zooplankton in EAS based on ADCP backscatter was consisting of three sites: Mumbai in NEAS, Goa in CEAS and Kollam in SEAS. The extended mooring sites are at Okha at NEAS, Jaigarh at CEAS, Udupi in the transition zone of CEAS & SEAS and Kanyakumari at SEAS is the southern most location in our study area.

ADCP data from three mooring sites were analysed from 2012 to 2020 in [Aparna et al., 2022]. They have fine-tuned the methodology to obtain backscatter and estimated zooplankton biomass from it using in situ volumetric zooplankton biomass data. A comparison is made in later paragraphs, since the methodology remains same in the current study and new time series data is available. The monthly climatology of biomass and ZSS is computed for all locations having valid data in 24 - 120 m depth range.

The high biomass regime in the upper ocean and low biomass regime in deeper depths is differentiated using the 215 $mg\ m^{-3}$ biomass contour. For simplicity, this biomass contour is abbreviated to be z215 and its depth is denoted as D215 henceforth; region lying above this contour is the upper ocean biomass. The choice of 215 $mg\ m^{-3}$ isn't abrupt; it is carefully chosen to accommodate the seasonal variation, as a shift to biomass contour lower than the z215 would be unviable as our data is only till 120 m depth. A higher biomass contour would lead to inferior view of the seasonal cycle such as in the case of Kanyakumari and Okha where D215 is often low enough to reach ∼20 - 30 m depths. The climatology of zooplankton biomass at different mooring location is discussed at locations northward starting from southern mooring location (Fig. 4).

3.1 Southern EAS

At Kanyakumari, during March to May, the zooplankton biomass is restricted to top layer ($\sim$ 30 m) as inferred from D215 (Fig. 4 g1). A thin layer of low biomass is seen from mid-May to late-June which divides the upper layer biomass to three distinct regions; a low biomass layer sandwiched between layers of higher biomass. With the advent of summer monsoon, the depth of 23 ^{o} C isotherm (henceforth D23) shallows alongwith oxycline and a rise in biomass is observed. The D215 deepens reaching as deep as 60 m during June to September. It is sustained throughout the summer monsoon and begins to decline in October-November. Contrary to May-June biomass, we see a thin layer of high biomass ($\sim$ 35-50 m) in this period. This could be due to advection of biomass carried by the monsoon currents. During winter monsoon; the D215 shifts to shallower depths. A gradual increase is seen in the chlorophyll biomass starting from April and the peak is attained in June (Fig. 4 g2). The ZSS is increased in June, however the growth is minimal. There is almost no seasonal variation in ZSS off Kanyakumari (seasonal ZSS range, 1.56 $gm\ m^{-2}$) as compared to the ZSS variation at the nearest northern mooring site off Kollam (seasonal ZSS range, 4.09 $gm\ m^{-2}$), where a strong seasonal cycle is observed and the D215 is deeper for any given month. Off Kollam, higher biomass is present in the larger portion of water column and the D215 is at $\sim$ 110 m during Mar-May (Fig. 4. f1). Similar to Kanyakumari, the decrease in biomass with depth is gradual and there is presence of biomass below z215. The D215 begins to shallow with progressing summer monsoon. During this period, a sharp decrease is seen in the D23 ($\sim$ 60 m in June to September) while the oxycline (2.1 $ml\ L^{-1}$) overshoots the thermocline (Fig. 4. f1). A steep rise in chlorophyll biomass is seen off Kollam and its peak is attained in August. The ZSS declines in the same period and reaches a minimum when the chlorophyll biomass is at its peak. The chlorophyll biomass decreases rapidly in the following months, while the ZSS increases and a maxmimum is seen during October. This feature was earlier reported by [Aparna et al., 2022] showing disproportionate interaction between zooplankton and phytoplankton. This begs the question of existing understanding of predator - prey relationship in a local-scale ecological system. A similar feature is seen further north mooring site albeit with a relatively weaker zooplankton biomass, off Udupi which sits at the transition zone of SEAS & CEAS. The peak of chlorophyll and minimum of ZSS occurs in September (Fig. 4 e2) which one month later than off Kollam. The 2.1 $ml\ L^{-1}$ Oxygen contour overshoots thermocline, however it reaches to a much shallow depth of $\sim$ 20 m. The D215 closely followes D23 from late June to November, and it is shallower for rest of the year.

3.2 Central EAS

Off Goa, the D215 seasonal trend is similar to Udupi but it is entirely restricted by D23 & oxycline that closely followes it. During March-May, the D215 is at $\sim$ 100 m which shallows with onset of summer monsoon; the chlorophyll biomass increases during this period and the maximum occurs in August afterwhich the chlrophyll biomass and ZSS both decrease in September. Although we witness an increase in chlorophyll biomass in October, the D215 is restricted to the $\sim$ 50 m in this period (fig. 4d1) and the ZSS is at it minimum (fig. 4d2) similar to what is observed off Udupi and Kollam. The ZSS rapidly increases and reaches its maximum in January, sustained till March and then gradually declines. Unlike the previous locations, the biomass off Goa decreases rapidly below the z215 as reported earlier [Aparna et al., 2022], reaching as low as 60 $mg\ m^{-3}$ during June to September at 130 m.

The ZSS off Jaigarh is identical but stronger to that of off Goa, owing to an higher biomass above z215 and the comparatively deeper D215. The D215 is restricted by D23 & oxycline for most of the year and it only exceeds during October-December(Fig. 4c1). From the ZSS maximum in February, it steadily decreases and attains a minimum in September (coincides with lower D215), a rapid rise is seen in the following months. What's intriguing is a presence of strong seasonal cycle in ZSS off Jaigarh (7.52 $gm\ m^{-2}$, highest among all locations) although the seasonal variation in Chlorophyll biomass (Fig. 4c2) is visibly non-existent (0.55 $mg\ m^{-3}$, lowest among all locations). This is an exact opposite scenario of Kanyakumari mooring site, where an insignificant seasonal variation in ZSS (1.56 $gm\ m^{-2}$) is seen even though the chlorophyll biomass varies strongly (1.61 $mg\ m^{-3}$). Starting from Kollam (Fig. 4f1) and moving northward to Jaigarh (Fig. 4c1), we see that the core of high zooplankton biomass gradually shifts from summer monsoon (off Kollam) to winter monsson (off Jaigarh), with the trasition of upper ocean zooplankton biomass happening along Udupi and Goa.

3.3 Northern EAS

Further north of Jaigarh, off Mumbai the D215 follows a similar pattern i.e, a deeper D215 in December to early April, resulting in a higher ZSS in the same period (Fig. 4b2). The D23 off Mumbai follows D215 and the oxycline follows an erratic pattern, reaching depths $>$ 140 during January to March (Fig. 4b1); when a higher biomass is observed above z215. The chlorophyll biomass shows seasonal variation albeit lower than the SEAS counterpart. Its peak occurs in August, then decreases rapidly and increases from October onwards maintaining the biomass at 0.5 $mg\ m^{-3}$ till March. In zooplankton biomass climatology, during September-October a thin layer of low biomass regime is see at depths $\sim$30 - 40 m, combined with shallow D215 leading to the ZSS minimum. The ZSS increases rapidly from its minima in October in the following month as the D215 deepens and the maximum occurs in February. The chlorophyll biomass decreases from

March and a gradual decrease in ZSS is seen till July, after which the ZSS bascally flattens even though the chlorophyll increases.

At the northernmost site of EAS i.e, off Okha, a noticeable feature is deeper oxycline, exceeding > 140m from February to late May while the D215 is at a shallow depth of 80m for the same period, while D23 lies inbetween at $\sim$ 100m. The biomass above z215 is much weaker compared to Mumbai as seen in the zooplankton biomass climatology owing to a shallower D215 which leads to a lower ZSS. From April onwards a low biomass layer is seen at the upper ocean $\sim$20-40 m which extends till Late November. For this period, a high zooplankton biomass layer is sandwiched between two low biomass layer, similar to Mumbai zooplankton biomass in September-October. There's two chlorophyll biomass maxima off Okha; one in February [Keerthi et al., 2017] and the other during August in summer monsoon [Lévy et al., 2007]. The ZSS remains flat in June to September although the chlorphyll biomass increases period. Afterwards, ZSS gradually increases and attains its maximum in February same as the chlorophyll biomass. The ZSS sustains this maximum till March, declines rapidly in April and then gradually till July.

3.4 Comparison to previous result

A comparison with the zooplankton biomass and standing stock climatology of previous work [Aparna et al., 2022] is made in this section for the locations of Mumbai, Goa and Kollam. In the previous study data from 2012 to 2020 is used, while the present study includes data 2017 to 2023.

The D215 is shallower at all locations and as a result a lower ZSS is seen in the climatology of the present study (Fig. 5). The difference in D215 is prominent off Goa; while in the previous climatology (Fig. 5b1), the D215 is deeper and lies along D23, in the present climatological data (Fig. 5b2), The D215 is shallower and lies $\sim$ 20 - 40 m above the D23 during January to April; and a relatively lower biomass is present above z215. This goes same for the biomass off Mumbai (Fig. 5a1 & 5a2) i.e, a comparatively shallow D215 and lower ZSS in comparison with [Aparna et al., 2022]. Off Kollam, a higher biomass is observed from May to June in previous study, while in the present study, along with May to June a higher biomass is seen from September to November(Fig 5c2) which is reflected as a minima of ZSS occuring in August (Fig. 5d2). The higher ZSS on either side to this minima is less pronounced in previous data. Chlorophyll biomass shows stronger peak for all locations in August in present study, when the zooplankton-phytoplankton relationship discrepancy is observed off Kollam similar to results reported in previous climatology.

3.5 The seasonal cycle of biomass

The seasonal cycle of zooplankton of these seven location is described in this section.

A preliminary analysis of the biomass time series in daily and monthly averaged scale shows that the biomass decreases with increasing depth (Fig. 3) at all the seven locations.

The rate of biomass decrease with depth, roughly defined as the difference between the mean biomass at 40 m and 105 m depth, is highest off Jaigarh and Mumbai as it has higher biomass in upper ocean (Fig. 3,c2,b2). This is followed by CEAS locations Goa and Udupi. While the rate of biomass decrease is lower off Kollam for 2017 to 2020. The rate of decrease is lowest off Okha and Kanyakumari. Written in the order of their rate of decrease from the difference of biomass: Jaigarh (96 $mg\ m^{-3}$), Mumbai (91 $mg\ m^{-3}$), Okha (79 $mg\ m^{-3}$), Udupi (78 $mg\ m^{-3}$), Kollam(73 $mg\ m^{-3}$), Goa (72 $mg\ m^{-3}$) and Kanyakumari (39 $mg\ m^{-3}$). The weaker decline in zooplankton biomass with respect to the depth at Okha (Fig. 3.a1,a2) at NEAS is agreeing with earlier reported data Madhupratap et al. [2001], Smith and Madhupratap [2005], Wishner et al. [1998] where oxygen deficit at is thought to be the cause. The sites at SEAS, especially off Kanyakumari and 2017 to

2020 off Kollam also have weaker decline [Madhupratap et al., 2001, Aparna et al., 2022]. However, after 2020 the rate of decline in biomass with depth off Kollam is similar to that off Mumbai in stark contrast to its previous years. This is due to a strong bloom in these years also seen at other locations. This high growth led to increase in biomass in the entire water column(Fig. 3.f1,f2).

Analysis of the D215 shows strong seasonality at the CEAS moorings off Goa and Jaigarh, with low variation in biomass in its upper ocean, with shallow (deeper) D215 in summer (winter) monsoon. This is followed by the moorings at transition zone off Mumbai (NEAS) and Udupi (SEAS). The

include wavelet analysis results

References

Anna-Karin Almén and Tobias Tamelander. Temperature-related timing of the spring bloom and match between phytoplankton and zooplankton. *Marine Biology Research*, 16(8-9):674–682, 2020.

P Amol, D Shankar, V Fernando, A Mukherjee, SG Aparna, R Fernandes, GS Michael, ST Khalap, NP Satelkar, Y Agarvadekar, et al. Observed intraseasonal and seasonal variability of the west india coastal current on the continental slope. *Journal of Earth System Science*, 123(5):1045–1074, 2014.

P Amol, Suchandan Bemal, D Shankar, V Jain, V Thushara, V Vijith, and PN Vinayachandran. Modulation of chlorophyll concentration by downwelling rossby waves during the winter monsoon in the southeastern arabian sea. *Progress in Oceanography*, 186:102365, 2020.

SG Aparna, DV Desai, D Shankar, AC Anil, Shrikant Dora, and R Khedekar. Seasonal cycle of zooplankton standing stock inferred from adcp backscatter measurements in the eastern arabian sea. *Progress in Oceanography*, 203: 102766, 2022.

Carin J Ashjian, Sharon L Smith, Charles N Flagg, and Nasseer Idrisi. Distribution, annual cycle, and vertical migration of acoustically derived biomass in the arabian sea during 1994–1995. *Deep Sea Research Part II: Topical Studies in Oceanography*, 49(12):2377–2402, 2002.

K Banse and DC English. Geographical differences in seasonality of czcs-derived phytoplankton pigment in the arabian sea for 1978–1986. *Deep Sea Research Part II: Topical Studies in Oceanography*, 47(7-8):1623–1677, 2000.

Karl Banse. Hydrography of the arabian sea shelf of india and pakistan and effects on demersal fishes. In *Deep sea research and oceanographic Abstracts*, volume 15, pages 45–79. Elsevier, 1968.

Karl Banse. Zooplankton: pivotal role in the control of ocean production: I. biomass and production. *ICES Journal of marine Science*, 52(3-4):265–277, 1995.

WE Barraclough, RJ LeBrasseur, and OD Kennedy. Shallow scattering layer in the subarctic pacific ocean: detection by high-frequency echo sounder. *Science*, 166(3905):611–613, 1969.

H. P. Batchelder, J. R. VanKeuren, R. D. Vaillancourt, and E. Swift. Spatial and temporal distributions of acoustically estimated zooplankton biomass near the marine light-mixed layers station (59°30'n, 21°00'w) in the north atlantic in may 1991. *Journal of Geophysical Research: Oceans*, 100:6549–6563, 1995. doi: 10.1029/94jc00981.

John C Brock and Charles R McClain. Interannual variability in phytoplankton blooms observed in the northwestern arabian sea during the southwest monsoon. *Journal of Geophysical Research: Oceans*, 97(C1):733–750, 1992.

John C Brock, Charles R McClain, Mark E Luther, and William W Hay. The phytoplankton bloom in the northwestern arabian sea during the southwest monsoon of 1979. *Journal of Geophysical Research: Oceans*, 96(C11): 20623–20642, 1991.

Abhisek Chatterjee, D Shankar, SSC Shenoi, GV Reddy, GS Michael, M Ravichandran, VV Gopalkrishna, EP Rama Rao, TVS Udaya Bhaskar, and VN Sanjeevan. A new atlas of temperature and salinity for the north indian ocean. *Journal of Earth System Science*, 121:559–593, 2012.

Anya Chaudhuri, D Shankar, SG Aparna, P Amol, V Fernando, A Kankonkar, GS Michael, NP Satelkar, ST Khalap, AP Tari, et al. Observed variability of the west india coastal current on the continental slope from 2009–2018. *Journal of Earth System Science*, 129(1):57, 2020.

Anya Chaudhuri, P Amol, D Shankar, S Mukhopadhyay, SG Aparna, V Fernando, and A Kankonkar. Observed variability of the west india coastal current on the continental shelf from 2010–2017. *Journal of Earth System Science*, 130:1–21, 2021.

Boris Cisewski, Volker H Strass, Monika Rhein, and Sören Krägefsky. Seasonal variation of diel vertical migration of zooplankton from adcp backscatter time series data in the lazarev sea, antarctica. *Deep Sea Research Part I: Oceanographic Research Papers*, 57(1):78–94, 2010.

Kent L Deines. Backscatter estimation using broadband acoustic doppler current profilers. In *Proceedings of the IEEE Sixth Working Conference on Current Measurement (Cat. No. 99CH36331)*, pages 249–253. IEEE, 1999.

A Edvardsen, D Slagstad, KS Tande, and P Jaccard. Assessing zooplankton advection in the barents sea using underway measurements and modelling. *Fisheries Oceanography*, 12(2):61–74, 2003.

S Fielding, G Griffiths, and HSJ Roe. The biological validation of adcp acoustic backscatter through direct comparison with net samples and model predictions based on acoustic-scattering models. *ICES Journal of Marine Science*, 61(2):184–200, 2004.

Charles N Flagg and Sharon L Smith. On the use of the acoustic doppler current profiler to measure zooplankton abundance. *Deep Sea Research Part A. Oceanographic Research Papers*, 36(3):455–474, 1989.

Kevin D. Friedland, Charles A. Stock, Kenneth F. Drinkwater, Jason S. Link, Robert T. Leaf, Burton Shank, Julie M. Rose, Cynthia H. Pilskaln, and Michael J. Fogarty. Pathways between primary production and fisheries yields of large marine ecosystems, 2012.

Charles H Greene, Peter H Wiebe, Chris Pelkie, Mark C Benfield, and Jacqueline M Popp. Three-dimensional acoustic visualization of zooplankton patchiness. *Deep Sea Research Part II: Topical Studies in Oceanography*, 45 (7):1201–1217, 1998.

Charles F Greenlaw. Acoustical estimation of zooplankton populations 1. *Limnology and Oceanography*, 24(2): 226–242, 1979.

Davide Guerra, Katrin Schroeder, Mireno Borghini, Elisa Camatti, Marco Pansera, Anna Schroeder, Stefania Sparnocchia, and Jacopo Chiggiato. Zooplankton diel vertical migration in the corsica channel (north-western mediterranean sea) detected by a moored acoustic doppler current profiler. *Ocean Science*, 15(3):631–649, 2019.

Graeme C Hays. A review of the adaptive significance and ecosystem consequences of zooplankton diel vertical migrations. In *Migrations and Dispersal of Marine Organisms: Proceedings of the 37 th European Marine Biology Symposium held in Reykjavík, Iceland, 5–9 August 2002*, pages 163–170. Springer, 2003.

PJ Herring, MJR Fasham, AR Weeks, JCP Hemmings, HSJ Roe, PR Pugh, S Holley, NA Crisp, and MV Angel. Across-slope relations between the biological populations, the euphotic zone and the oxygen minimum layer off the coast of oman during the southwest monsoon (august, 1994). *Progress in Oceanography*, 41(1):69–109, 1998.

Karen J Heywood, S Scrope-Howe, and ED Barton. Estimation of zooplankton abundance from shipborne adcp backscatter. *Deep Sea Research Part A. Oceanographic Research Papers*, 38(6):677–691, 1991.

Laura Hobbs, Neil S Banas, Jonathan H Cohen, Finlo R Cottier, Jørgen Berge, and Øystein Varpe. A marine zooplankton community vertically structured by light across diel to interannual timescales. *Biology Letters*, 17(2): 20200810, 2021.

Raleigh R Hood, Lynnath E Beckley, and Jerry D Wiggert. Biogeochemical and ecological impacts of boundary currents in the indian ocean. *Progress in Oceanography*, 156:290–325, 2017.

Ryuichiro Inoue, Minoru Kitamura, and Tetsuichi Fujiki. Diel vertical migration of zooplankton at the s 1 biogeochemical mooring revealed from acoustic backscattering strength. *Journal of Geophysical Research: Oceans*, 121 (2):1031–1050, 2016.

Songnian Jiang, Tommy D Dickey, Deborah K Steinberg, and Laurence P Madin. Temporal variability of zooplankton biomass from adcp backscatter time series data at the bermuda testbed mooring site. *Deep Sea Research Part I: Oceanographic Research Papers*, 54(4):608–636, 2007.

R Jyothibabu, NV Madhu, H Habeebrehman, KV Jayalakshmy, KKC Nair, and CT Achuthankutty. Re-evaluation of 'paradox of mesozooplankton'in the eastern arabian sea based on ship and satellite observations. *Journal of Marine Systems*, 81(3):235–251, 2010.

Myounghee Kang, Sunyoung Oh, Wooseok Oh, Dong-Jin Kang, SungHyun Nam, and Kyounghoon Lee. Acoustic characterization of fish and macroplankton communities in the seychelles-chagos thermocline ridge of the southwest indian ocean. *Deep Sea Research Part II: Topical Studies in Oceanography*, 213:105356, 2024.

Madhavan Girijakumari Keerthi, Matthieu Lengaigne, Marina Levy, Jerome Vialard, Vallivattathillam Parvathi, Clément de Boyer Montégut, Christian Ethé, Olivier Aumont, Iyyappan Suresh, Valiya Parambil Akhil, et al. Physical control of interannual variations of the winter chlorophyll bloom in the northern arabian sea. *Biogeosciences*, 14(15):3615–3632, 2017.

Corinne Le Qu, Robbie M Andrew, Josep G Canadell, Stephen Sitch, Jan Ivar Korsbakken, Glen P Peters, Andrew C Manning, Thomas A Boden, Pieter P Tans, Richard A Houghton, et al. Global carbon budget 2016. *Earth System Science Data*, 8(2):605–649, 2016.

Marina Lévy, D Shankar, J-M André, SSC Shenoi, Fabien Durand, and Clément de Boyer Montégut. Basin-wide seasonal evolution of the indian ocean's phytoplankton blooms. *Journal of Geophysical Research: Oceans*, 112 (C12), 2007.

M Li, A Gargett, and K Denman. What determines seasonal and interannual variability of phytoplankton and zooplankton in strongly estuarine systems? *Estuarine, Coastal and Shelf Science*, 50(4):467–488, 2000.

Yanliang Liu, Jingsong Guo, Yuhuan Xue, Chalermrat Sangmanee, Huiwu Wang, Chang Zhao, Somkiat Khokiattiwong, and Weidong Yu. Seasonal variation in diel vertical migration of zooplankton and micronekton in the andaman sea observed by a moored adcp. *Deep Sea Research Part I: Oceanographic Research Papers*, 179:103663, 2022.

M Madhupratap, P Haridas, Neelam Ramaiah, and CT Achuthankutty. Zooplankton of the southwest coast of india: abundance, composition, temporal and spatial variability in 1987. 1992.

M Madhupratap, TC Gopalakrishnan, P Haridas, KKC Nair, PN Aravindakshan, G Padmavati, and Shiney Paul. Lack of seasonal and geographic variation in mesozooplankton biomass in the arabian sea and its structure in the mixed layer. *Current science. Bangalore*, 71(11):863–868, 1996a.

M Madhupratap, S Prasanna Kumar, PMA Bhattathiri, M Dileep Kumar, S Raghukumar, KKC Nair, and N Ramaiah. Mechanism of the biological response to winter cooling in the northeastern arabian sea. *Nature*, 384(6609): 549–552, 1996b.

M Madhupratap, TC Gopalakrishnan, P Haridas, and KKC Nair. Mesozooplankton biomass, composition and distribution in the arabian sea during the fall intermonsoon: implications of oxygen gradients. *Deep Sea Research Part II: Topical Studies in Oceanography*, 48(6-7):1345–1368, 2001.

PA Maheswaran, G Rajesh, C Revichandran, and KKC Nair. Upwelling and associated hydrography along the west coast of india during southwest monsoon, 1999. 2000.

JP McCreary, Raghu Murtugudde, Jerome Vialard, PN Vinayachandran, Jerry D Wiggert, Raleigh R Hood, D Shankar, and S Shetye. Biophysical processes in the indian ocean. *Indian Ocean biogeochemical processes and ecological variability*, 185:9–32, 2009.

Julian P McCreary Jr, Pijush K Kundu, and Robert L Molinari. A numerical investigation of dynamics, thermodynamics and mixed-layer processes in the indian ocean. *Progress in Oceanography*, 31(3):181–244, 1993.

Donald C McNaught. Acoustical determination of zooplankton distribution. In *Proc. 11th Conf. Great lakes Res.*, pages 76–84, 1968.

A Mukherjee, D Shankar, V Fernando, P Amol, SG Aparna, R Fernandes, GS Michael, ST Khalap, NP Satelkar, Y Agarvadekar, et al. Observed seasonal and intraseasonal variability of the east india coastal current on the continental slope. *Journal of Earth System Science*, 123(6):1197–1232, 2014.

S Mukhopadhyay, D Shankar, SG Aparna, A Mukherjee, V Fernando, A Kankonkar, S Khalap, NP Satelkar, MG Gaonkar, AP Tari, et al. Observed variability of the east india coastal current on the continental slope during 2009–2018. *Journal of Earth System Science*, 129:1–22, 2020.

Jerry Mullison. Backscatter estimation using broadband acoustic doppler current profilers-updated. In *Proceedings of the ASCE Hydraulic Measurements & Experimental Methods Conference, Durham, NH, USA*, pages 9–12, 2017.

KKC Nair, M Madhupratap, TC Gopalakrishnan, P Haridas, and Mangesh Gauns. The arabian sea: physical environment, zooplankton and myctophid abundance. 1999.

PV Nair. Primary productivity in the indian seas. *CMFRI Bulletin*, 22:1–63, 1970.

Lingyun Nie, Jianchao Li, Hao Wu, Wenchao Zhang, Yongjun Tian, Yang Liu, Peng Sun, Zhenjiang Ye, Shuyang Ma, and Qinfeng Gao. The influence of ocean processes on fine-scale changes in the yellow sea cold water mass boundary area structure based on acoustic observations. *Remote Sensing*, 15(17):4272, 2023.

MD Ohman and H-J Hirche. Density-dependent mortality in an oceanic copepod population. *Nature*, 412(6847): 638–641, 2001.

G Padmavati, P Haridas, KKC Nair, TC Gopalakrishnan, P Shiney, and M Madhupratap. Vertical distribution of mesozooplankton in the central and eastern arabian sea during the winter monsoon. *Journal of Plankton Research*, 20(2):343–354, 1998.

MR Patil, CP Ramamirtham, P Udaya Varma, and CP Nair. Hydrography of the west coast of india during the pre-monsoon period of the year 1962. *Journal of marine biological association of India*, 6(1):151–164, 1964.

Richard Edward Pieper. *A study of the relationship between zooplankton and high-frequency scattering of underwater sound*. PhD thesis, University of British Columbia, 1971.

SA Piontkovski, R Williams, and TA Melnik. Spatial heterogeneity, biomass and size structure of plankton of the indian ocean: some general trends. *Marine ecology progress series*, pages 219–227, 1995.

Emmanuel Potiris, Constantin Frangoulis, Alkiviadis Kalampokis, Manolis Ntoumas, Manos Pettas, George Petihakis, and Vassilis Zervakis. Acoustic doppler current profiler observations of migration patternsof zooplankton in the cretan sea. *Ocean Science*, 14(4):783–800, 2018.

SZ Qasim. Biological productivity of the indian ocean. 1977.

CP Ramamirtham and AVS Murty. Hydrography of the west coast of india during the pre-monsoon period of the year 1962—part 2: in and offshore waters of the konkan and malabar coasts. *Journal of the Marine Biological Association of India*, 7(1):150–168, 1965.

S Ramamurthy. Studies on the plankton of the north kanara coast in relation to the pelagic fishery. *Journal of Marine Biological Association of India*, 7(1):127–149, 1965.

Mehbuba Rehim and Mudassar Imran. Dynamical analysis of a delay model of phytoplankton–zooplankton interaction. *Applied Mathematical Modelling*, 36(2):638–647, 2012.

T. P. Rippeth and J. H. Simpson. Diurnal signals in vertical motions on the hebridean shelf. *Limnology and Oceanography*, 43:1690–1696, 1998. doi: 10.4319/lo.1998.43.7.1690.

John H Ryther, John R Hall, Allan K Pease, Andrew Bakun, and Mark M Jones. Primary organic production in relation to the chemistry and hydrography of the western indian ocean 1. *Limnology and Oceanography*, 11(3): 371–380, 1966.

D Sameoto and S Paulowich. The use of 120 khz sonar in zooplankton studies. In *OCEANS'77 Conference Record*, pages 523–528. IEEE, 1977.

D Shankar and SR Shetye. On the dynamics of the lakshadweep high and low in the southeastern arabian sea. *Journal of Geophysical Research: Oceans*, 102(C6):12551–12562, 1997.

D Shankar, R Remya, PN Vinayachandran, Abhisek Chatterjee, and Ambica Behera. Inhibition of mixed-layer deepening during winter in the northeastern arabian sea by the west india coastal current. *Climate Dynamics*, 47:1049–1072, 2016.

D Shankar, R Remya, AC Anil, and V Vijith. Role of physical processes in determining the nature of fisheries in the eastern arabian sea. *Progress in Oceanography*, 172:124–158, 2019.

SR Shetye and AD Gouveia. Coastal circulation in the north indian ocean: Coastal segment (14, sw). John Wiley and Sons, New York, USA, 1998.

SR Shetye, AD Gouveia, SSC Shenoi, GS Michael, D Sundar, AM Almeida, and K Santanam. The coastal current off western india during the northeast monsoon. *Deep Sea Research Part A. Oceanographic Research Papers*, 38 (12):1517–1529, 1991.

SR Shetye, AD Gouveia, and SSC Shenoi. Does winter cooling lead to the subsurface salinity minimum off saurashtra, india? *Oceanography of the Indian Ocean*, pages 617–625, 1992.

Greg M Silsbe, Michael J Behrenfeld, Kimberly H Halsey, Allen J Milligan, and Toby K Westberry. The cafe model: A net production model for global ocean phytoplankton. *Global Biogeochemical Cycles*, 30(12):1756–1777, 2016.

Houssem Smeti, Marc Pagano, Christophe Menkes, Anne Lebourges-Dhaussy, Brian PV Hunt, Valerie Allain, Martine Rodier, Florian De Boissieu, Elodie Kestenare, and Cherif Sammari. Spatial and temporal variability of zooplankton off n ew c aledonia (s outhwestern p acific) from acoustics and net measurements. *Journal of Geophysical Research: Oceans*, 120(4):2676–2700, 2015.

SL Smith and M Madhupratap. Mesozooplankton of the arabian sea: patterns influenced by seasons, upwelling, and oxygen concentrations. *Progress in Oceanography*, 65(2-4):214–239, 2005.

R Subrahmanyan. Studies on the phytoplankton of the west coast of india: Part ii. physical and chemical factors influencing the production of phytoplankton, with remarks on the cycle of nutrients and on the relationship of the phosphate-content to fish landings. In *Proceedings/Indian Academy of Sciences*, volume 50, pages 189–252. Springer, 1959.

R Subrahmanyan and AH Sarma. Studies on the phytoplankton of the west coast of india. part iii. seasonal variation of the phytoplankters and environmental factors. *Indian Journal of Fisheries*, 7(2):307–336, 1960.

Laura Ursella, Vanessa Cardin, Mirna Batistić, Rade Garić, and Miroslav Gačić. Evidence of zooplankton vertical migration from continuous southern adriatic buoy current-meter records. *Progress in oceanography*, 167:78–96, 2018.

Laura Ursella, Sara Pensieri, Enric Pallàs-Sanz, Sharon Z Herzka, Roberto Bozzano, Miguel Tenreiro, Vanessa Cardin, Julio Candela, and Julio Sheinbaum. Diel, lunar and seasonal vertical migration in the deep western gulf of mexico evidenced from a long-term data series of acoustic backscatter. *Progress in Oceanography*, 195:102562, 2021.

V Vijith, PN Vinayachandran, V Thushara, P Amol, D Shankar, and AC Anil. Consequences of inhibition of mixed-layer deepening by the west india coastal current for winter phytoplankton bloom in the northeastern arabian sea. *Journal of Geophysical Research: Oceans*, 121(9):6583–6603, 2016.

Peter H Wiebe, Charles H Greene, Timothy K Stanton, and Janusz Burczynski. Sound scattering by live zooplankton and micronekton: empirical studies with a dual-beam acoustical system. *The Journal of the Acoustical Society of America*, 88(5):2346–2360, 1990.

Monika Winder and Daniel E Schindler. Climatic effects on the phenology of lake processes. *Global change biology*, 10(11):1844–1856, 2004.

Karen F Wishner, Marcia M Gowing, and Celia Gelfman. Mesozooplankton biomass in the upper 1000 m in the arabian sea: overall seasonal and geographic patterns, and relationship to oxygen gradients. *Deep Sea Research Part II: Topical Studies in Oceanography*, 45(10-11):2405–2432, 1998.

Table 1: ADCP deployment details at the locations. The temporal resolution is 1 hour, bin size(vertical resolution) 4 m. All ADCPs are operated at 153.3 kHz. The moorings are at a water column depth of 950 - 1200 m on the continental slope and are serviced on yearly basis according to ship availability. The 6th column consists of Reference echo intensity (Er) for each beam, while the 7th column contains the corresponding RSSI conversion factor [Deines, 1999].

	Date		Depth			
Station (Position; ^{o}E,^{o}N)	Deployment	Recovery	Ocean	ADCP	Er	Kc
Okha (67.47, 22.26)	01/10/2018	01/12/2019	996	118	37 , 37 , 37 , 36	0.42 , 0.44 , 0.42 , 0.43
	01/12/2019	04/12/2020	1166	312	39 , 36 , 38 , 36	0.42 , 0.44 , 0.42 , 0.43
	04/12/2020	08/03/2022	1021	144	41 , 37 , 38 , 37	0.42 , 0.44 , 0.42 , 0.43
	08/03/2022	01/01/2023	1019	142	37 , 38 , 39 , 36	0.42 , 0.44 , 0.42 , 0.43
Mumbai (69.24, 20.01)	09/11/2017	29/09/2018	1025	150	36 , 34 , 39 , 42	0.40 , 0.40 , 0.40 , 0.40
	29/09/2018	29/11/2019	1122	125	35 , 36 , 39 , 42	0.40 , 0.40 , 0.40 , 0.40
	29/11/2019	02/12/2020	1143	164	37 , 34 , 39 , 43	0.40 , 0.40 , 0.40 , 0.40
	02/12/2020	06/03/2022	1125	142	36 , 34 , 39 , 42	0.40 , 0.40 , 0.40 , 0.40
	07/03/2022	02/01/2023	1103	158	37 , 34 , 40 , 43	0.40 , 0.40 , 0.40 , 0.40
Jaigarh (71.12, 17.53)	27/10/2017	27/09/2018	1039	198	32 , 35 , 33 , 32	0.45 , 0.45 , 0.45 , 0.45
	27/09/2018	30/10/2019	1032	164	32 , 35 , 33 , 31	0.45 , 0.45 , 0.45 , 0.45
	03/11/2019	30/11/2020	1142	264	32 , 36 , 33 , 32	0.45 , 0.45 , 0.45 , 0.45
	30/11/2020	05/03/2022	1099	119	33 , 36 , 34 , 32	0.45 , 0.45 , 0.45 , 0.45
	03/04/2022	26/06/2022	1120	136	68 , 71 , 69 , 66	0.45 , 0.45 , 0.45 , 0.45
Goa (72.74, 15.17)	03/10/2017	25/09/2018	1000	174	35 , 37 , 34 , 35	0.44 , 0.44 , 0.40 , 0.41
	25/09/2018	16/10/2019	969	145	38 , 36 , 36 , 34	0.44 , 0.44 , 0.40 , 0.41
	16/10/2019	29/11/2020	966	143	44 , 38 , 36 , 43	0.44 , 0.44 , 0.40 , 0.41
	29/11/2020	03/03/2022	985	157	35 , 40 , 35 , 38	0.44 , 0.44 , 0.40 , 0.41
	03/03/2022	05/01/2023	984	159	35 , 38 , 35 , 34	0.44 , 0.44 , 0.40 , 0.41
Udupi (74.04, 12.5)	05/10/2017	06/10/2018	1028	176	44 , 46 , 29 , 35	0.45 , 0.45 , 0.45 , 0.45
	06/10/2018	18/10/2019	1027	179	32 , 38 , 30 , 36	0.45 , 0.45 , 0.45 , 0.45
	18/10/2019	11/12/2020	1018	168	33 , 37 , 31 , 38	0.45 , 0.45 , 0.45 , 0.45
	11/03/2022	06/01/2023	1036	155	31 , 32 , 32 , 33	0.45 , 0.45 , 0.45 , 0.45
Kollam (75.44, 9.05)	07/10/2017	08/10/2018	1174	200	43 , 55 , 45 , 43	0.49 , 0.50 , 0.49 , 0.50
	08/10/2018	20/10/2019	1160	123	49 , 62 , 46 , 46	0.49 , 0.50 , 0.49 , 0.50
	20/10/2019	13/12/2020	1209	176	52 , 61 , 54 , 55	0.49 , 0.50 , 0.49 , 0.50
	13/12/2020	13/03/2022	1129	91	49 , 51 , 46 , 47	0.49 , 0.50 , 0.49 , 0.50
	13/03/2022	08/01/2023	1149	164	41 , 48 , 43 , 41	0.49 , 0.50 , 0.49 , 0.50
Kanyakumari (77.39,6.96)	16/11/2016	08/10/2017	1096	252	37 , 36 , 37 , 37	0.42 , 0.44 , 0.42 , 0.43
	08/10/2017	10/10/2018	1055	181	32 , 34 , 38 , 35	0.45 , 0.45 , 0.45 , 0.45
	10/10/2018	22/10/2019	1075	180	36 , 34 , 39 , 36	0.45 , 0.45 , 0.45 , 0.45
	22/10/2019	14/12/2020	1060	167	33 , 35 , 36 , 35	0.45 , 0.45 , 0.45 , 0.45
	14/12/2020	14/03/2022	1184	287	34 , 36 , 36 , 35	0.45 , 0.45 , 0.45 , 0.45
	14/03/2022	10/01/2023	1069	172	33 , 36 , 42 , 36	0.45 , 0.45 , 0.45 , 0.45

Table 2:
Volumetric samples of zooplankton of various stations. The tags corresponds to cruise and particular station. The sampling depth range is standardised for later years for bin range of 0-25m, 25-50m, 50-75m, 75-100m, 100-150m

Sample number	Tag	Lat(^{o}N)	Lon(^{o}E)	Date	Time (IST)	Sampling depth range (m)
1-3	G1	15.18	72.79	25 Sep 18	452	50–25, 100–50, 150–100
4-6	G2	15.16	72.71	25 Sep 18	2108	50–25, 100–50, 150–100
7-10	G2	15.16	72.71	25 Sep 18	2137	40–20, 60–40, 80–60, 100–80
11-14	J1			26 Sep 18	2000	40–20, 60–40, 80–60, 100–80
15-17	J2			27 Sep 18	2000	50–25, 100–50, 150–100
18-21	J2			27 Sep 18	2100	40–20, 60–40, 80–60, 100–80
22-25	M1	20	69.19	28 Sep 18	2135	40–20, 60–40, 80–60, 100–80
26-27	M1	20	69.19	28 Sep 18	2205	50–25, 100–50
28-29	M2	20.01	69.2	29 Sep 18	2035	50–25, 100–50
30-33	M2	20.01	69.2	29 Sep 18	2057	40–20, 60–40, 80–60, 100–80
34-37	U1			5 Oct 18	2000	40–20, 60–40, 80–60, 100–80
38-40	U1			5 Oct 18	2100	50–25, 100–50, 150–100
41-43	U2			6 Oct 18	2000	50–25, 100–50, 150–100
44-47	U2			6 Oct 18	2100	40–20, 60–40, 80–60, 100–80
48-51	K1	9.06	75.42	8 Oct 18	421	40–20, 60–40, 80–60, 100–80
52-54	K1	9.06	75.42	8 Oct 18	449	50–25, 100–50, 150–100
55-56	K2	9.04	75.4	8 Oct 18	2027	50–25, 100–50
57-60	K2	9.04	75.4	8 Oct 18	2045	40–20, 60–40, 80–60, 100–80
61-64	G2	15.16	72.74	16 Oct 19	829	50–25, 75–50, 100–75, 150–100
65-67	G3	15.16	72.74	16 Oct 19	1812	50–25, 75–50, 100–75
68-70	K2	9.02	75.42	20 Oct 19	840	50–25, 75–50, 100–75
71-74	K3	9.04	75.43	20 Oct 19	1934	50–25, 75–50, 100–75, 150–100
75-78	KK1			22 Oct 19	742	50–25, 75–50, 100–75, 150–100
79-82	KK2			22 Oct 19	1925	50–25, 75–50, 100–75, 150–100
83-86	J1			30 Oct 19	324	50–25, 75–50, 100–75, 150–100
87-89	J2			4 Nov 19	946	75–50, 100–75, 150–100
90-92	M2	19.98	69.22	29 Nov 19	1434	50–25, 75–50, 100–75
93-96	M3	20.01	69.23	30 Nov 19	958	50–25, 75–50, 100–75, 150–100
97-100	O1	22.24	67.49	1 Dec 19	937	50–25, 75–50, 100–75, 150–100
101	O2	22.25	67.46	1 Dec 19	1957	150-100
102-105	G3	15.68	73.22	28 Nov 20	930	50–25, 75–50, 100–75, 150–100
105-108	G4	15.32	73.22	29 Nov 20	1558	50–25, 75–50, 100–75, 150–100
108-110	J2	17.85	71.21	30 Nov 20	1458	75–50, 100–75, 150–100
111-114	J3	17.91	71.21	1 Dec 20	1052	50–25, 75–50, 100–75, 150–100
115-118	M4	20.03	69.38	2 Dec 20	2016	50–25, 75–50, 100–75, 150–100
119.00	O2	22.41	67.8	4 Dec 20	953	150-100
120-123	O3	22.41	67.79	4 Dec 20	2011	50–25, 75–50, 100–75, 150–100
124-127	K3	9.11	75.72	12 Dec 20	2335	50–25, 75–50, 100–75, 150–100
128-131	K4	9.06	75.74	13 Dec 20	1507	50–25, 75–50, 100–75, 150–100
132-134	KK1	7.62	77.63	14 Dec 20	1226	50–25, 75–50
135-138	KK2	7.62	77.63	14 Dec 20	2047	50–25, 75–50, 100–75, 150–100
139-142	G4	15.32	73.21	3 Mar 22	823	50–25, 75–50, 100–75, 150–100
143-146	G5	15.68	73.21	4 Mar 22	1030	50–25, 75–50, 100–75, 150–100
147-150	M5	19.99	69.23	7 Mar 22	957	50–25, 75–50, 100–75, 150–100
151-154	O3	22.24	67.5	8 Mar 22	806	50–25, 75–50, 100–75, 150–100
155-158	U3	12.5	74.04	12 Mar 22	1156	50–25, 75–50, 100–75, 150–100
159-160	K4	9.04	75.42	13 Mar 22	1027	50–25, 75–50, 100–75
161-164	KK3	6.97	77.4	15 Mar 22	1220	50–25, 75–50, 100–75, 150–100

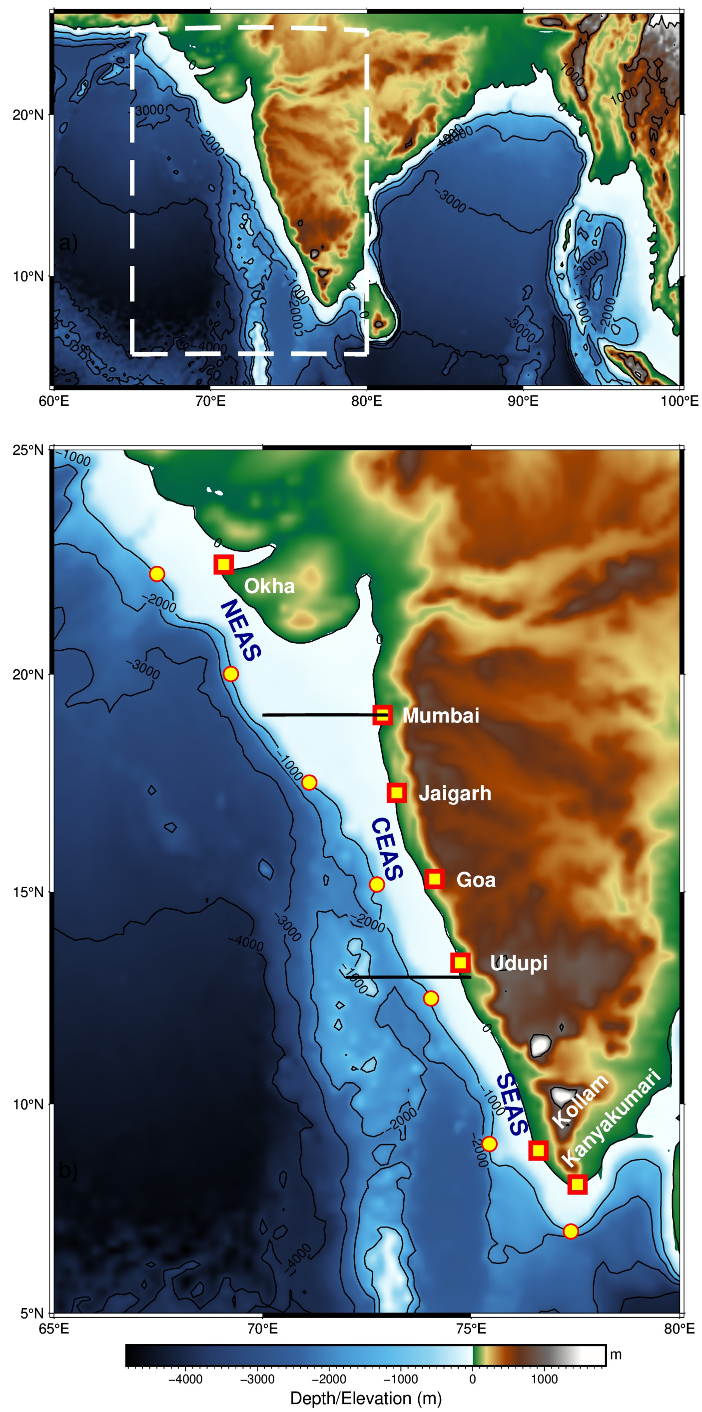

Figure 1: Map showing region of interest. The slope moorings are deployed at 1000 m depth.

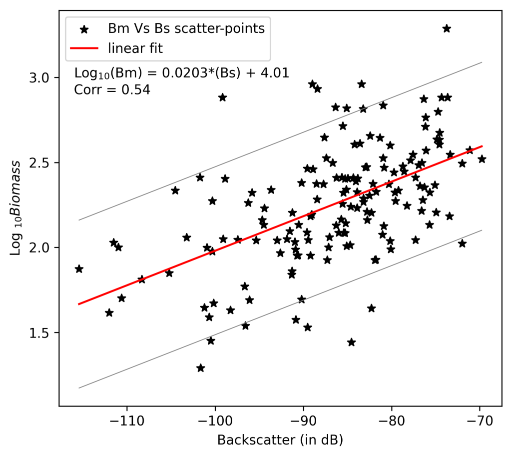

Figure 2: The linear fit line of Biomass (taken in log of biomass) and Backscatter. The linear fit line is within the error range of previous result of [Aparna et al., 2022] onto which latest zooplankton volumetric sample data is added.

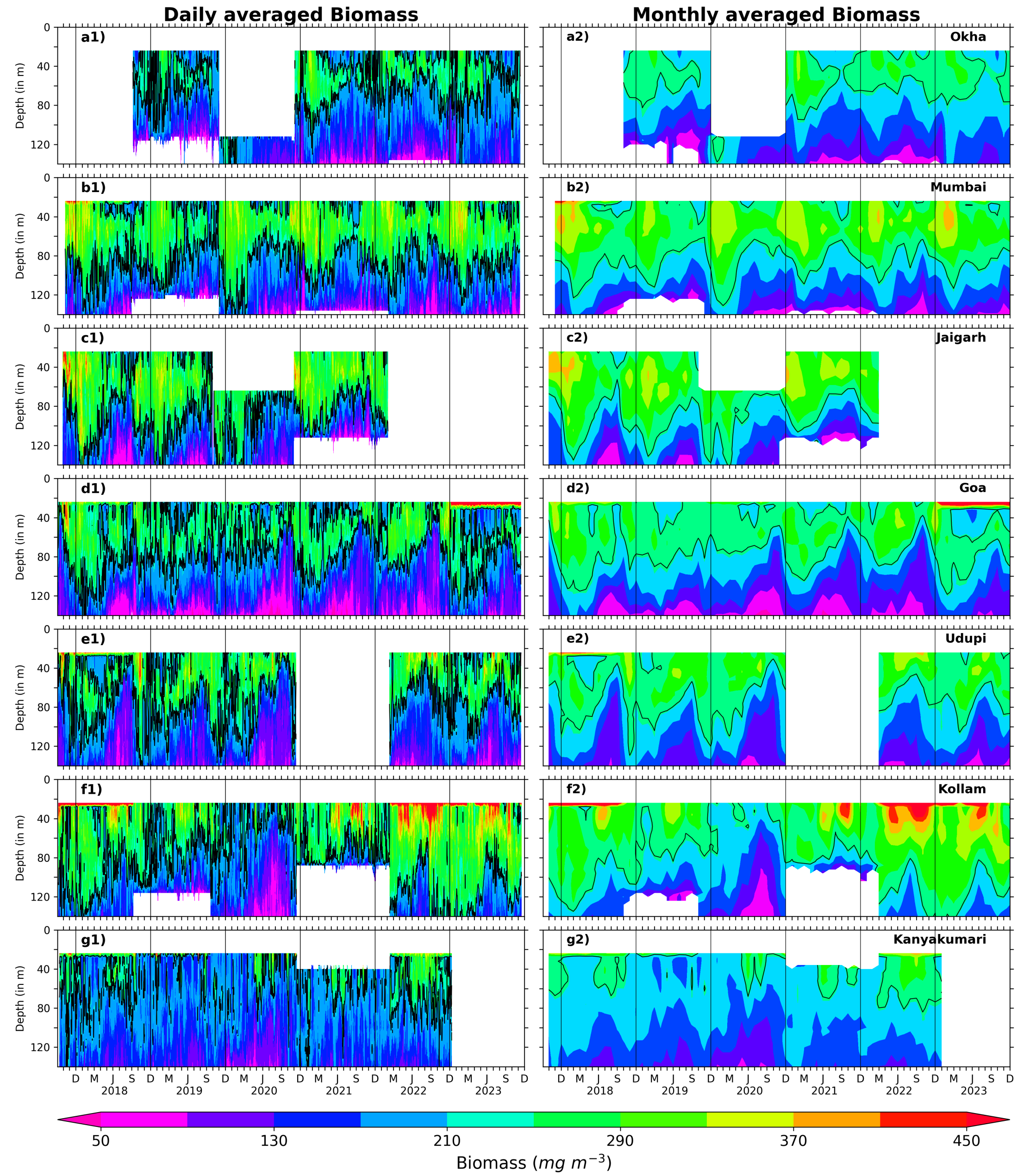

Figure 3: The Daily and monthly averaged biomass for EAS moorings, north (top) to south (bottom). The black contours are marking 215 $mg\ m^{-3}$ biomass.

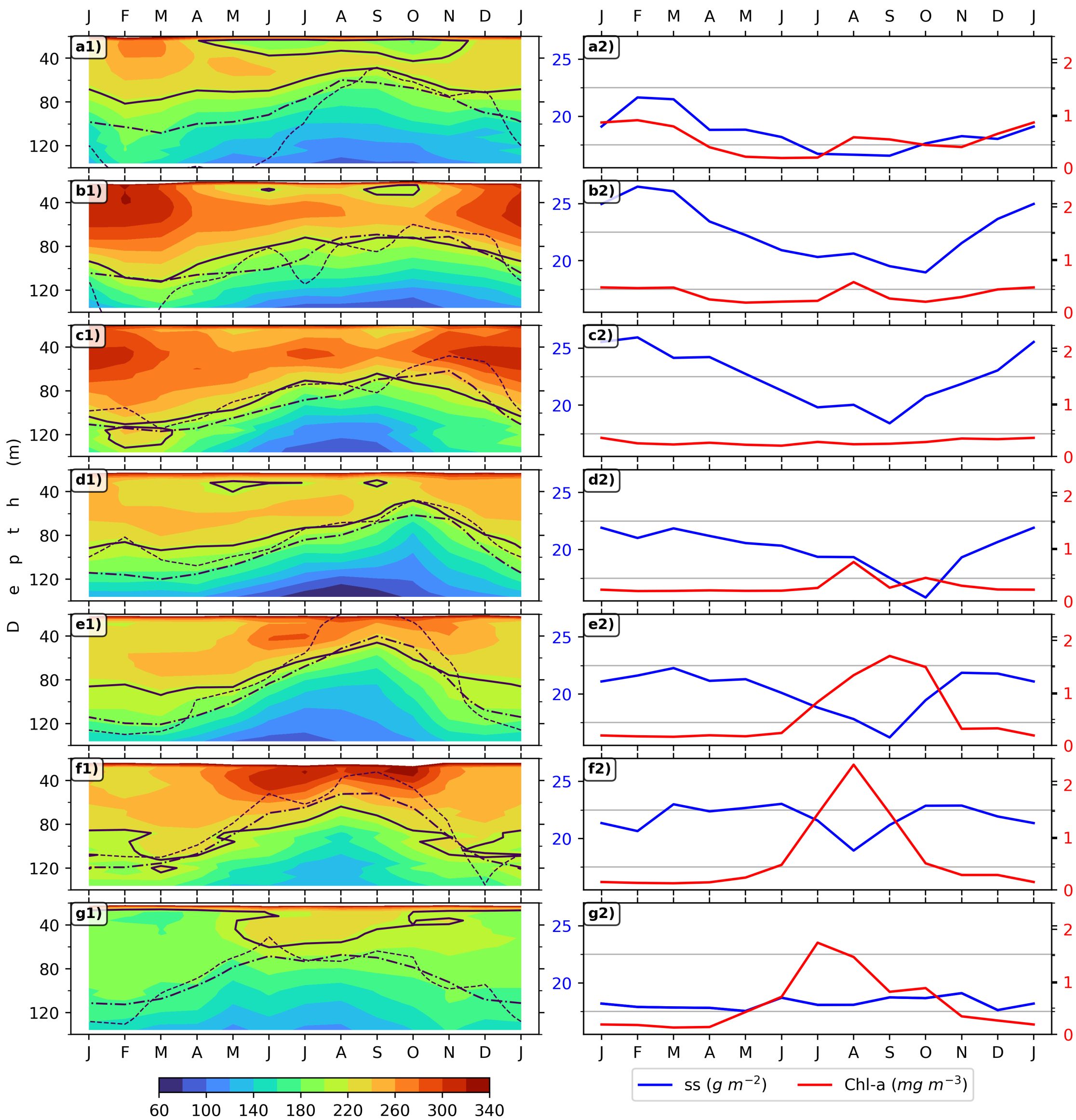

Figure 4: Monthly climatology of zooplankton biomass is shown in left panels for 7 locations, (bottom is southward). The D215 is shown in solid line. Dashed (dotted) line represents the depth of 23 ^{o}C (2.1 $ml\ L^{-1}$ oxygen)contour. The plot labels are as follows: a1 & a2 for Okha, b1 & b2 for Mumbai, c1 & c2 for Jaigarh, d1 & d2 for Goa, e1 & e2 for Udupi, f1 & f2 for Kollam, g1 & g2 for Kanyakumari. The right panel is zooplankton standing stock and chlorophyll climatology for respective location.

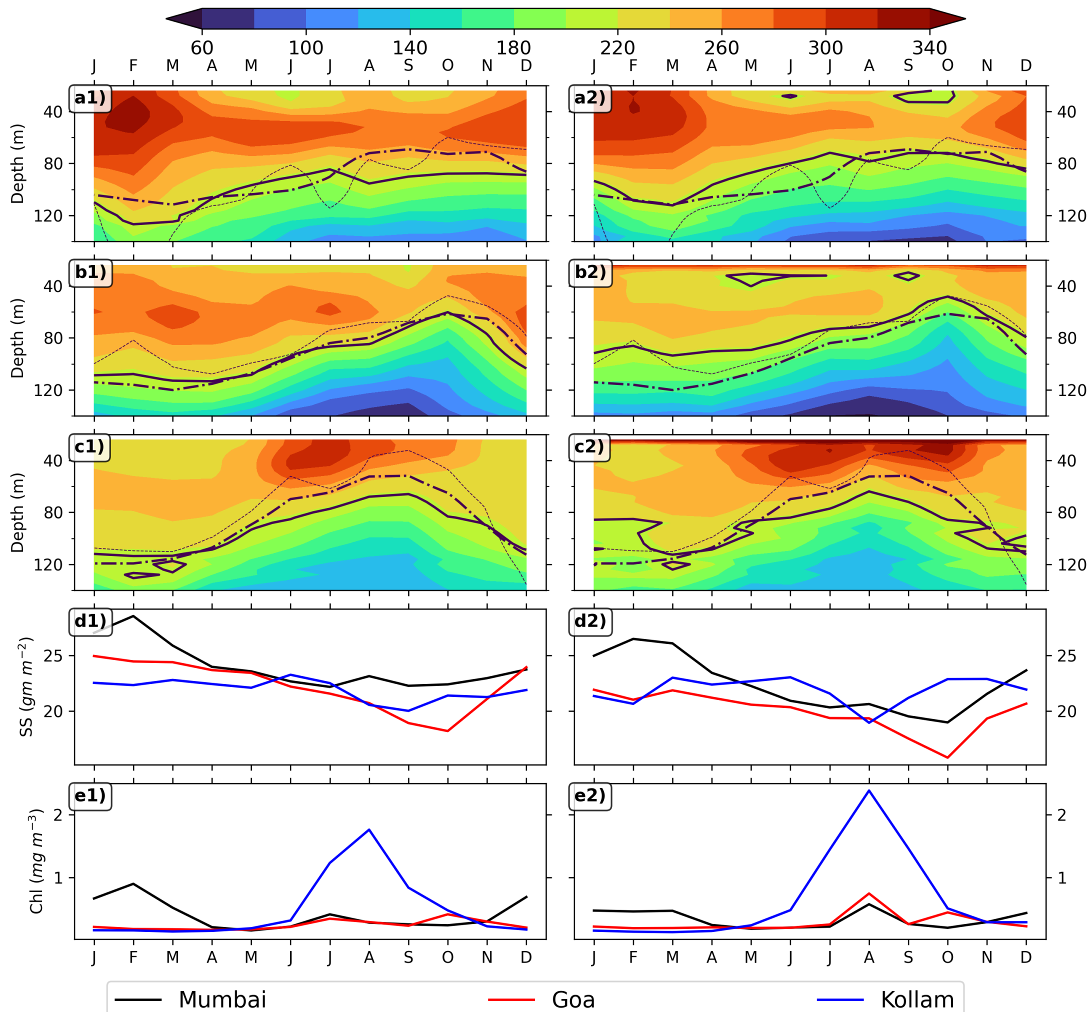

Figure 5: Monthly climatology of zooplankton biomass is shown in left panels for 3 locations which were earlier used in [Aparna et al., 2022]; a1, b1 & c1 is the biomass climatology for Mumbai, Goa and Kollam, d1 is for climatological zooplankton standing stock, e1 is chlorophyll biomass climatology; a2, b2, c2, d2 & e2 is same but based on data from 2017 to 2023. The D215 is shown in solid line. Dashed (dotted) line represents the depth of 23 ^{o}C (2.1 $ml\ L^{-1}$ oxygen) contour.

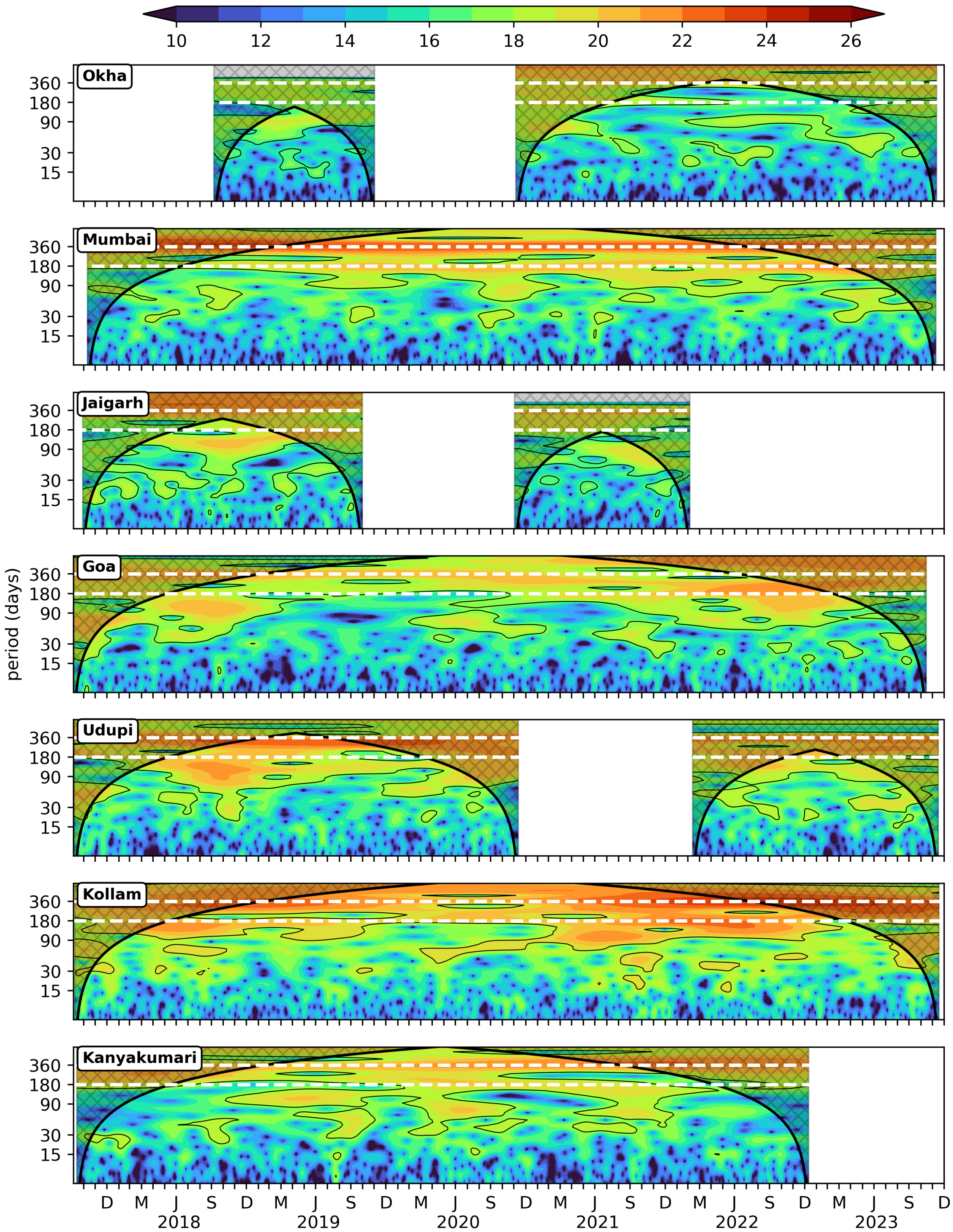

Figure 6: Wavelet power spectra (Morlet) of the 40 m zooplankton biomasss plotted against time as abscissa and period in days as ordinate. The wavelet power is in $\log_2$ scale, the 95 % significance is marked in black contours; the cross-shaded region falls under cone of influence.

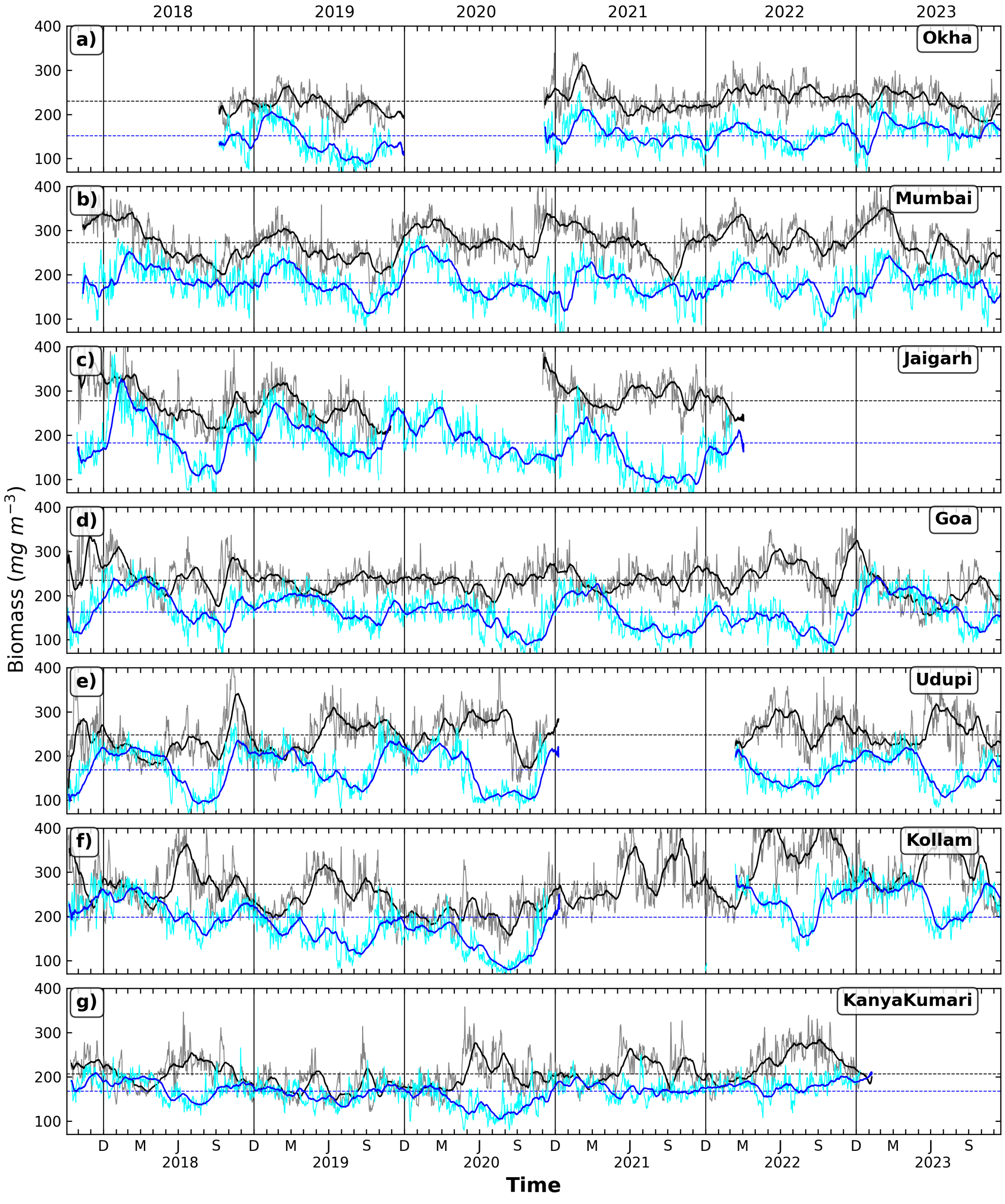

Figure 7: The daily biomass at depth of 40 m and 104 m for all locations shown by grey and cyan curves. The black and blue lines shows the 30 day rolling averaged biomass.